

## A Simulation Modelling of Inductive/Non-inductive Current Ramp-up at Slow Rate for Low $I_i$ , High Vertical Stability

Y. Nakamura<sup>1)</sup>, H. Fujieda<sup>2)</sup>, N. Takei<sup>2)</sup>, S. Miyamoto<sup>2)</sup>, Y. Kusama<sup>2)</sup> and R. Yoshino<sup>2)</sup>

1) Nippon Advanced Technology Co., Ltd., Ibaraki, 319-1112, Japan

2) Japan Atomic Energy Agency Ibaraki, 311-0193, Japan

### 1. Introduction

In tokamak fusion reactors with superconducting PF coil system, ramping-up of the plasma current for startup of discharges is essentially restrained at a rate much slower than the current tokamak with normal PF conductors. Therefore, the induced plasma current can penetrate deeply into the core region with higher electron temperature, *i.e.* low Ohmic resistivity, leading to a centrally peaked current profile. Consequently, such the high  $I_i$ , highly elongated configuration imperative to divertor formation has a dangerous property of causing vertical instability. Meanwhile, the centrally peaked current profile lower  $q_0$  on magnetic axis, leading to sawtooth activity that could reduce the current ramp-efficiency. Additional heating at early phase of the ramp-up has been addressed as one of startup procedures that retard the penetration of plasma current. A potential drawback, however, is the substantial increase of direct heat load to limiter.

The paper presents a comprehensive simulation modelling of the stable plasma current ramp-up at a slow rate, based on the ITER 15 MA inductive Scenario 2 [1,]. Using TSC [2], a self-consistent simulation, including a model for improved core energy confinement, non-inductive current sources, has been performed in consideration of sawtooth-free condition,  $q_{\min} \geq 2$  to avoid internal MHD activity in reversed shear plasmas and flux consumption that could seriously compromise the available duration of the burn phase. Phasing of the earliest possible formation of a diverted plasma, formation of internal transport barrier (ITB), transition from L to H-mode, timing of the heating and non-inductive current driving using off-axis EC current drive (CD) source are discussed.

### 2. Simulation modelling

Using TSC, operation scenarios which attain the target plasma current of 15 MA from 0.4 MA with buildup time of 100 sec, *e.g.* ITER 15MA inductive scenario 2, were examined. Our prime interest is attached to see how the external control means: (a) *self-generated bootstrap (BS) current after L to H-mode transition*; (b) *additional heating to retard current penetration*; (c) *off-axis ECCD* meet the operation and physics requirements for slow 15 MA ramp-up:  $q_0 > 1$  for sawtooth stability, engineering limit of  $I_{PF6} < 17.5$  MA, lower  $I_i$ -operation for vertical stability ( $I_i \ll 1.2$ ), high ramp-efficiency for saving OH flux ( $C_{Ejima} \sim 0.4$ ), Plasma shaping control ( $\kappa_{95} < 1.8$ ), and early X-point formation for reducing heat load to limiter structure.

Axisymmetric MHD fluid dynamics was obtained by solving the momentum equation with Faraday's law and Ohm's law. The transport coefficients are given by as a sum of the turbulent term  $\chi_{CDBM}$  based on the self-sustained turbulence theory [3] and the neoclassical term  $\chi_{NC}$ . The CDBM is the L-mode based, turbulent transport model, involving the effect of the improved core confinement in accordance with the local magnetic shear. In weak or negative magnetic shear region, the anomalous transport is significantly reduced to enhance the local pressure gradient, resulting in an ITB-formation. To model an edge transport barrier (ETB) of H-mode, the neoclassical transport was assumed in a prescribed edge-region ( $\rho > 0.9$ ). An off-axis deposition profiles of the NB-heating and the external CD using 170 GHz EC source are also given as fixed ones for the sake of simplicity. BS current was provided by the model of Hirshman and Sigmar. The plasma density was controlled by feedback.

### 3. TSC simulation of inductive/non-inductive current ramp-up

#### 3.1. (a) Plain inductive ramp and L to H-mode transition by high power NB heating

Figure 1 shows the current ramp-up, starting from an outboard-limited plasma of  $I_p = 0.4$  MA, positioned on midplane:  $Z_p = 0$  m. An early X-point was formed at  $I_p \sim 4.5$  MA,  $t \sim 22$  s. Subsequently, the plasma with bottom divertor was vertically moved back to  $Z_p \sim 0.5$  m of the nominal equilibrium position. As long as the plain inductive ramp lasts, the internal inductance  $l_i$  continued to increase till  $t \sim 78$  s. When  $l_i$  reached unity, high power NB heating of  $P_{NB} \sim 27$  MW started in order to intentionally cause an L to H-mode transition. Ohmic power was  $P_{OH} \sim 10$  MW, and hence, total power for plasma heating was  $\sim 37$  MW. Here, the threshold power needed for the L/H transition was estimated at  $P_{L/H} \sim 30$  MW, using the transition threshold of  $P_{L/H} = 2.84 M^{-1} B_T^{0.82} n_e^{0.58} R^{1.00} a^{0.81}$ . As denoted by the oval sign in Fig. 1, a remarkable change of  $l_i$ , i.e.  $\delta l_i \sim -0.3$ , was observed after the L/H transition. In the case without the L/H transition,  $l_i$  still further continued to increase up to  $\sim 1.2$  at  $t \sim 100$  s. Figure 2 shows time-evolutions of toroidal current density  $j_\phi$  and toroidal loop voltage  $V_{loop}$ . A strong edge structure of H-mode appears in the  $j_\phi$  profile after the L/H transition, generating a large BS current around the pedestal ( $\rho > 0.9$ ). According to the remarkable  $l_i$ -change shown

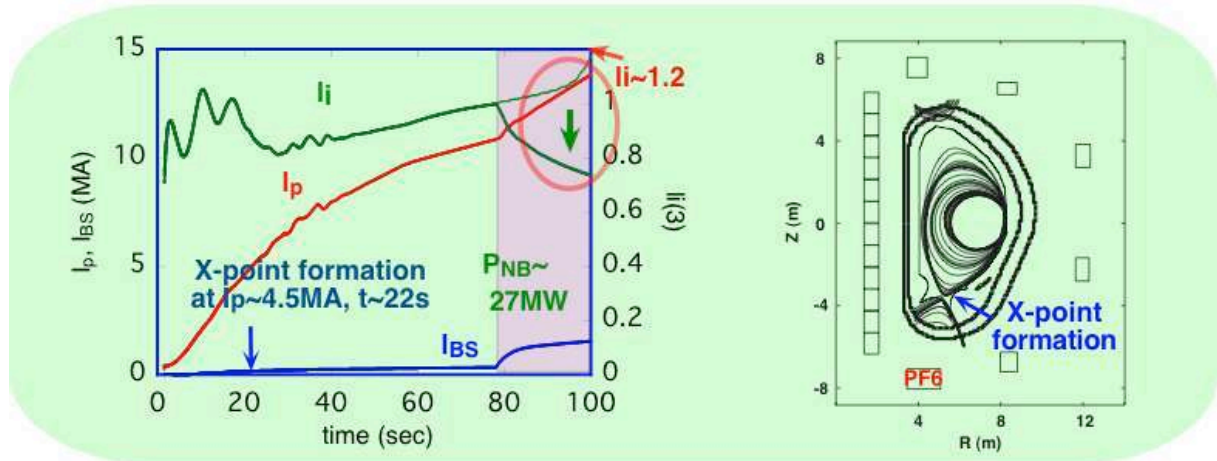


Fig. 1. Current ramp-up from  $I_p = 0.4$  MA,  $Z_p = 0$  m. Early X-point formation at  $I_p \sim 4.5$  MA,  $t \sim 22$  s. During inductive ramp,  $l_i$  continued to increase till  $t \sim 78$  s. NB heating of  $P_{NB} \sim 27$  MW with Ohmic power of  $P_{OH} \sim 10$  MW started to cause L to H-mode transition, while the L/H transition threshold was  $P_{L/H} \sim 30$  MW. As denoted by the oval sign, a remarkable change of  $l_i$ , i.e.  $\delta l_i \sim -0.3$ , was observed after L/H transition. In the case of inductive ramp without L/H transition,  $l_i$  increased up to  $\sim 1.2$  at  $t \sim 100$  s.

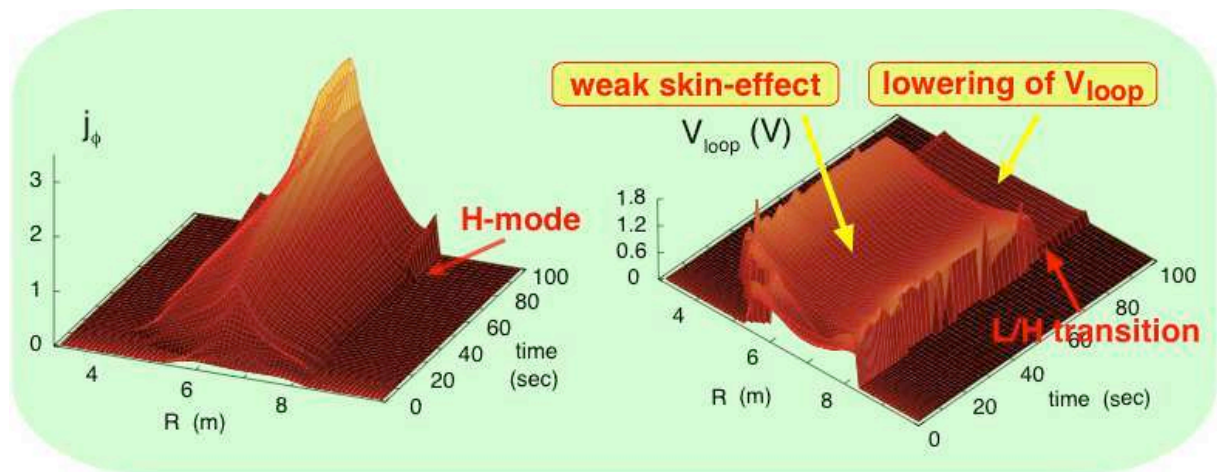


Fig. 2. Time-evolutions of toroidal current density  $j_\phi$  and toroidal loop voltage  $V_{loop}$ . A strong edge  $j_\phi$  structure of H-mode appears after L/H transition, generating a large BS current around  $\rho > 0.9$ . Emergence of edge BS current greatly lowers  $V_{loop}$ , leading to the remarkable  $l_i$ -lowering. Consequently, peaking of  $j_\phi$  profile eventually ceased after L/H transition.

in Fig. 1, the peaking of the  $j_\phi$  profile eventually ceased after the L/H transition. It follows that once the L to H-mode transition occurs, an emergence of the non-inductive, edge BS current greatly lowers  $V_{loop}$ , leading to the remarkable  $l_i$ -lowering, hence vertical stability. Additionally, the edge BS current improves ramp-efficiency:  $C_{Ejima} \sim 0.65$ , while  $C_{Ejima} \sim 0.8$  without the L/H transition. Unfortunately, plasma shape control after the L/H transition, however, becomes extremely difficult, because the drastic  $l_i$ -change to  $\sim 0.7$  alters the plasma elongation  $\kappa$  up to  $\sim 1.9$ . In the present TSC simulation, PF6 coil current was beyond the engineering limit of  $I_{PF6} < 17.5$  MA.

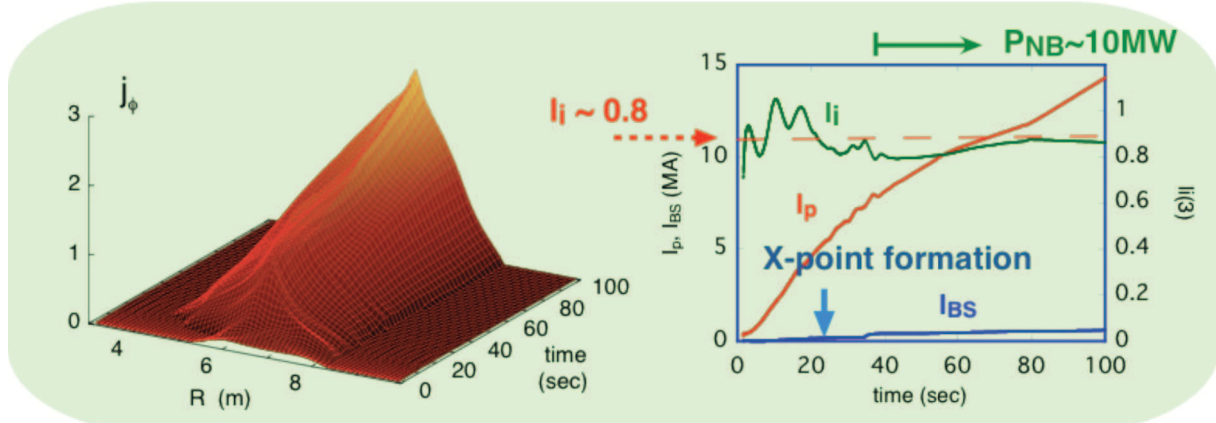


Fig. 3. Time-evolution of toroidal current density  $j_\phi$  and waveforms of plasma current  $I_p$ , BS current  $I_{BS}$  and internal inductance  $l_i$ .  $j_\phi$  profile becomes more flat than the plain inductive ramp, i.e.  $l_i$  remains  $\sim 0.8$ .

### 3.2. Inductive ramp with low power NB heating

An inductive current ramp scenario without L to H-mode transition was investigated. NB power of  $P_{NB} \sim 10$  MW less than the L/H transition threshold was applied 10 s after the X-point formation. Figure 3 shows time-evolution of toroidal current density  $j_\phi$ , together with waveforms of plasma current  $I_p$ , BS current  $I_{BS}$  and internal inductance  $l_i$ . Compared with the plain inductive ramp, the  $j_\phi$  profile becomes more flat, and hence  $l_i$  remains  $\sim 0.8$ . The NB heating retards penetration of the inductive current into the plasma core region. Figure 4 shows that the NB heating enhances a skin-effect on  $V_{loop}$  profile in a great deal, lowering  $V_{loop}$  by half. Furthermore, the shape control was fairly good, and the ramp-efficiency was allowable:  $C_{Ejima} \sim 0.55$ . Therefore, additional heating with lower power than  $P_{LH}$  ( $\sim 37$  MW) can provide one of possible operation modes for low  $l_i$  ( $\sim 0.8$ ), i.e. vertical stability, while avoiding L to H-mode formation. However, controllability of  $q_0$  was not acceptable, because  $q_0 < 1$  has been yet observed at the later phase of current ramp:  $t > 80$  s.

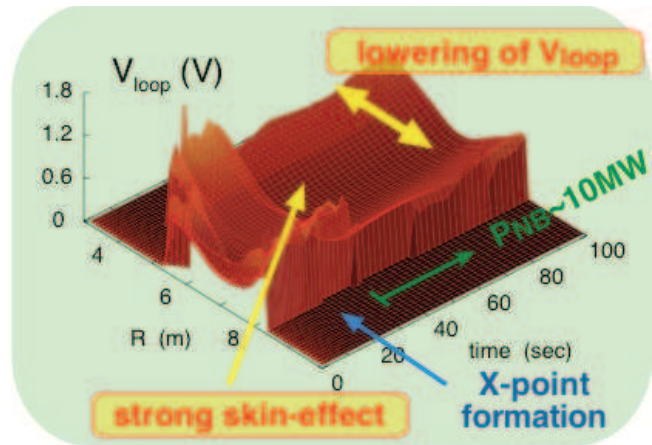


Fig. 4.  $V_{loop}$  profile of inductive ramp with low power NB heating, enhancing skin-effect while lowering  $V_{loop}$  in a great deal. lowering  $V_{loop}$  by half.

### 3.3. Inductive ramp with off-axis EC current drive

While avoiding the L/H transition, additional heating of  $P_{NB} \sim 5$  MW and  $P_{EC} \sim 5$  MW to raise electron temperature  $T_e$  and to drive off-axis EC current by  $I_{EC} \sim 1.5$  MA were applied 10 s after the X-point formation. Figure 5 shows time-evolution of  $j_\phi$ , together with waveforms of  $I_p$ , EC-driven current  $I_{EC}$ ,  $I_{BS}$  and  $l_i$ . Although the off-axis EC current increases,

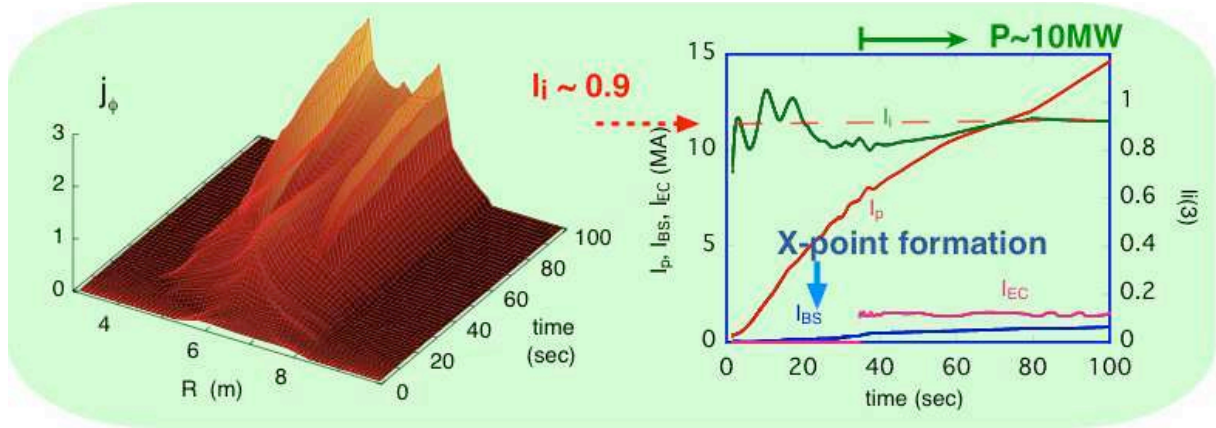


Fig. 5. Time-evolution of  $j_\phi$ ; waveforms of  $I_p$ , EC-driven current  $I_{EC}$ ,  $I_{BS}$  and  $l_i$  for the scenario without L/H transition and with  $P_{NB} \sim 5$  MW;  $P_{EC} \sim 5$  MW and off-axis  $I_{EC}$  of  $\sim 1.5$  MA. Although off-axis EC current increases, inductive current at mag. axis remained modest.  $l_i$  was low as  $\sim 0.9$ , and  $a_0 > 1$ .

the inductive current around magnetic axis remained modest. During the current ramp,  $l_i$  was kept low as  $\sim 0.9$ , and  $q_0 > 1$  remains over the ramp. As in the case of Fig. 4, time-evolution of  $V_{loop}$  profile, shown in Fig. 6, implies the heating with  $P_{NB}$  and  $P_{EC}$  enhances a skin-effect on  $V_{loop}$  profile in a great deal, retarding inductive current penetration. Note that the off-axis ECCD of  $\sim 1.5$  MA gives rise to a local dent structure of  $V_{loop}$ , hindering the inductive current from penetrating into the plasma core region. The shape control was fairly good as  $\kappa \sim 1.83$ , as well as the ramp-efficiency was kept as  $C_{Ejima} \sim 0.45$ .

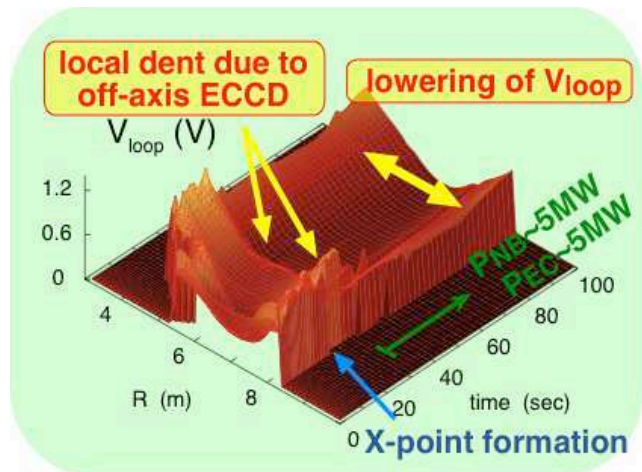


Fig. 6. Time-evolution of  $V_{loop}$ , implying  $P_{NB}$  and  $P_{EC}$  enhance skin-effect great deal, which retards inductive current penetration. Note that off-axis ECCD of 1.5 MA gives rise to local dent of  $V_{loop}$ , hindering penetration.

#### 4. Summary

Using TSC, inductive/non-inductive current ramp-up from  $I_p \sim 0.4$  to 15 MA were examined, demonstrating an early X-point formation at  $I_p \sim 4.5$  MA,  $t \sim 22$  s. Plain inductive ramp at a slow rate like ITER 15 MA inductive scenario 2 was shown to cause high- $l_i$  state ( $\sim 1.2$ ), leading to vertical instability.  $q_0$  was lowered ( $< 1$ ), leading to sawtooth activity, and hence the ramp-efficiency was reduced ( $C_{Ejima} \sim 0.8$ ).

From the point of view of establishing high vertical stability (low- $l_i$ ), sawtooth-free ( $q_0 > 1$ ), high efficiency (low- $C_{Ejima}$ ), external control means to tailor current profile: (a) L/H transition control, (b) additional heating, (c) off-axis ECCD were investigated. It was shown that (a) If L/H transition happens, the edge BS current reduces  $l_i$  too much, leading to failure of plasma shape control ( $I_{PF6} > 17.5$  MA). (b) Additional heating with lower power than  $P_{L/H}$  provides a lower  $l_i$ -operation for vertical stability ( $l_i \sim 0.8$ ) without H-mode. The ramp-efficiency was allowable:  $C_{Ejima} \sim 0.55$ . However,  $q_0$  remains less than unity. (c) Cooperating with additional heating, off-axis ECCD provides best scenario for high ramp-efficiency ( $C_{Ejima} \sim 0.45$ ), vertical stability ( $l_i \sim 0.9$ ) and sawtooth stability ( $q_0 > 1$ ).

[1] V. Lukash, et. al., Plasma Devices and Operations **15** (2007) 283.

[2] S.C. Jardin, N. Pomphery and J. Delucia, J. Comput. Phys. **66** (1986) 481.

[3] A. Fukuyama, et. al., Plasma Phys. Control. Fusion **37** (1995) 6611.